

# A Comparison of Piezoelectric Transformer AC/DC Converters with Current Doubler and Voltage Doubler Rectifiers

Gregory Ivensky, Svetlana Bronstein, and Shmuel (Sam) Ben-Yaakov, *Member, IEEE*

**Abstract**—The objective of this study was to develop recommendations for an optimal design of piezoelectric transformer (PT) ac/dc converters. The paper presents a comprehensive comparison of the two commonly used rectifier topologies in a PT based power converters: current doubler and voltage doubler rectifiers. The advantages and disadvantages of the two rectifiers were investigated and the range of their applications with respect to output current, voltage, power capability, load resistance etc.—was delineated. Generic parameters are proposed and used to derive normalized and closed form equations that can help choosing a PT for a given set of requirements. Simulation and experimental results were found to be in a good agreement with the derivation of the theoretical analysis.

**Index Terms**—Current doubler, piezoelectric transformer (PT) ac/dc converters, voltage doubler rectifiers.

## I. INTRODUCTION

AS PIEZOELECTRIC transformer (PT) technology is developing, PTs may become a viable alternative to electromagnetic transformers in various applications such as ac/dc converters. The problem of optimal PT converter design becomes, therefore, an important issue that needs to be addressed.

Two main types of rectifiers are generally applied at the output of PT ac/dc converters: the voltage doubler (VD) [Fig. 1(a)] and the current doubler (CD) [Fig. 1(b)]. In the VD, the average diodes' current is equal to the average load current while in the CD the diode's current is twice lower than the load current. On the other hand, the peak of the diodes' voltage in the VD is equal to the load voltage while in the CD the peak of the diodes' voltage is twice higher than the load voltage. Therefore, for high currents and low voltages (low resistance load) the CD rectifier is a superior choice, whereas for high voltages and low currents (high resistance load) the VD rectifier is a better choice. The problem is, however, that the load regions between these two rectification schemes are not well defined. This paper presents a comparative analysis of PT based power converters that apply these types of rectifiers.

The comparison methodology, applied in this study, follows the approach developed earlier [1]–[4] by which the output capacitor of PT and the rectifier sections are represented by an

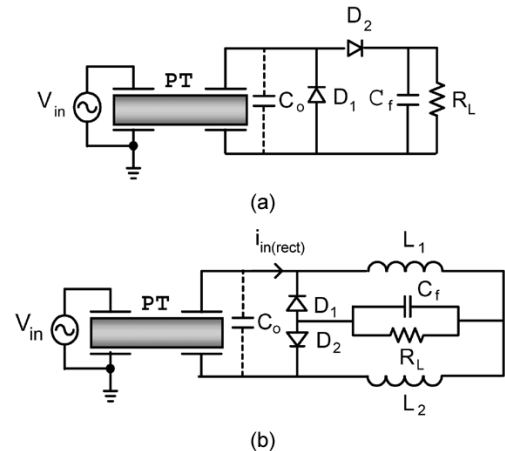


Fig. 1. Typical ac-dc PT power converter topologies: (a) voltage doubler rectifier and (b) current doubler rectifier.  $C_o$  is the output capacitance of the PT.

equivalent circuit. The equivalent circuit is linear and is composed of a parallel RC network that loads the PT as the corresponding rectifier does [2], [3]. The study applies the earlier generic analysis and generic characteristics of the PT [5] to carry out comparative analysis of the two types of rectifier, yielding a generic model of PT ac/dc power converters.

## II. COMPARATIVE CIRCUITS AND THE COMPARISON PRINCIPLES

It is assumed that both converters are operated at the maximum output voltage mode, that is, at the frequency that produces the maximum output voltage. As was shown earlier [3], [5], the frequency of maximum output is different from the mechanical resonant frequency. The principle of operation of the VD rectifier when operating at the maximum output voltage mode was studied in [3] and is further developed in the present work. Current doubler rectifier operating at the mechanical resonant frequency of PT was studied earlier [6] while the present work studies its operation at the maximum output voltage mode.

In order to generalize the model of the PT converter, we apply in this study the following normalized parameters.

Normalized load factor

$$K_{PT} = R_L/n^2 R_m \quad (1)$$

Normalized PT factor

$$A_{PT} = \omega_r C_o n^2 R_m \quad (2)$$

PT mechanical quality factor

$$Q_m = 1/(\omega_r C_r R_m) \quad (3)$$

Manuscript received August 5, 2003; revised March 2, 2004. This work was supported by the Israel Science Foundation Grant 113/02 and the Paul Ivanier Center for Robotics and Production Management. Recommended by Associate Editor R.-L. Lin.

The authors are with the Power Electronics Laboratory, Department of Electrical and Computer Engineering, Ben-Gurion University of the Negev, Beer-Sheva 84105, Israel (e-mail: sby@ee.bgu.ac.il).

Digital Object Identifier 10.1109/TPEL.2004.836646

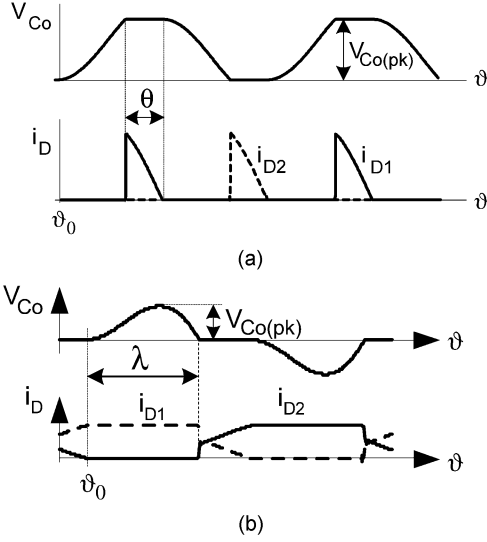


Fig. 2. Output voltage of the PT (across  $C_o$ ) and the diodes currents: (a) voltage doubler rectifier and (b) current doubler rectifier.

where  $R_L$  is the load resistance,  $R_m-L_r-C_r-C_o$  are the parameters of the equivalent circuit of PT;  $n$  is the PT's transfer ratio, and  $\omega_r = 1/\sqrt{L_r C_r}$  is the mechanical resonant frequency of the PT. These parameters refer to the elements of the conventional lumped model of a PT [3]–[5].

The normalized load factor  $K_{PT}$  is a convenient parameter to analyze the effect of the load resistance  $R_L$  on the operating conditions of the converter and rectifier (output voltage, power, efficiency). Analytical and experimental results presented below were obtained for a large  $K_{PT}$  range: from 0.5 up to  $3 \cdot 10^5$ .

The normalized PT parameter  $A_{PT}$  and the PT mechanical quality factor  $Q_m$  are independent of the load resistance. These parameters are useful for analyzing the operational conditions of the PT. In particular,  $A_{PT}$  can be used to obtain the dependence of the output voltage on the output capacitance of the PT,  $C_o$ . As clearly evident from the results of this study,  $C_o$  has a marked effect on the operation of the PT based converter. Analytical and experimental results presented below were obtained for a  $A_{PT}$  range of 0.01 up to 0.05 and varying  $Q_m$  from 50 up to 5000. It was found, however, that the effect of  $Q_m$  on the operational characteristics of the converter is insignificant when  $Q_m > 900$ .

The current and voltage waveforms of the two rectifiers that are compared in the study are presented in Fig. 2. The parameters marked in Fig. 2 are defined as follows:  $\vartheta = \omega t$  is the normalized time,  $\omega$  is the operating angular frequency,  $\theta$  is the duration of the VD rectifier input current pulses,  $\lambda$  is the duration of the CD rectifier input voltage pulses (i.e., the pulses of the PT output capacitor voltage).

Notwithstanding the fact that the output voltage of the PT in both converters  $v_{C_o}$  includes high harmonics components, the current waveform within the PT equivalent circuit ( $i_r$ ) is assumed to be sinusoidal due to the high quality factor of the resonant circuit. Consequently, power transfer to the output is affected only by the fundamental harmonics component. For that reason, both rectifiers can be studied by the first harmonics approximation. In both converters we replace the output capacitor

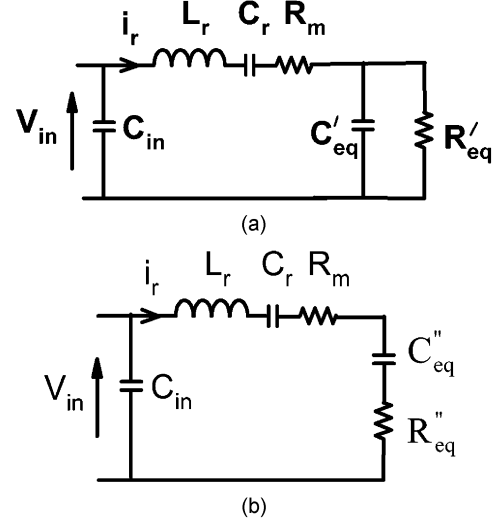


Fig. 3. Series-parallel (a) and series (b) equivalent circuits of a PT ac-dc converter reflected to the primary. The parallel  $C'_{eq}$  and  $R'_{eq}$  and series  $R''_{eq}$  and  $C''_{eq}$  networks emulate the loading effect of the rectifier ( $C'_{eq}$  includes the output capacitance of the PT- $C_o$ ).

of the PT and the loaded rectifier by an equivalent parallel network  $C_{eq}-R_{eq}$  (at the secondary side of PT). In the case of ideal and lossless rectifiers the values of the parameters can be derived from

$$\frac{V_{Co(1)pk}^2}{2R_{eq}} = \frac{V_L^2}{R_L} \quad (4)$$

$$C_{eq} = \frac{\tan \varphi(1)}{\omega R_{eq}} \quad (5)$$

where  $R_L$  is the load resistance,  $V_L$  is the load (dc) voltage,  $V_{Co(1)pk}$  is the peak of the first harmonics component of the capacitor  $C_o$  voltage  $v_{C_o}$ ,  $\varphi(1)$  is the phase angle between the voltage  $v_{C_o(1)}$  and the PT current  $i_r$  flowing through  $R_m-C_r-L_r$ .

Next we reflect this equivalent network to the primary where  $C'_{eq}-R'_{eq}$  are the reflected values [Fig. 3(a)] and  $C'_{eq} = C_{eq}n^2$ ,  $R'_{eq} = R_{eq}/n^2$ . This reflected parallel network is then converted to an equivalent series network  $C''_{eq}-R''_{eq}$  [Fig. 3(b)], [5] by applying the following relationships:

$$\begin{cases} R''_{eq} = R'_{eq} \cos^2 \varphi(1) \\ C''_{eq} = \frac{C'_{eq}}{\sin^2 \varphi(1)} \end{cases} \quad (6)$$

This presentation is used in the followings to obtain generalized expressions for the voltage ratio, power relationships, efficiency etc. in a similar form for the two converters. All expressions are normalized and apply per unit system.

#### A. Voltage Doubler Rectifier

Following [3], the duration of the impulses of the diodes' currents is  $\theta$  [Fig. 2(a)]

$$\theta = 2 \tan^{-1} \sqrt{\frac{2\pi}{\omega^* Q}} \quad (7)$$

where  $Q = \omega_r C_o R_L = A_{PT} K_{PT}$  is the PT load parameter,  $\omega^* = \omega/\omega_r$ , and  $\omega$  is the operating frequency corresponding to

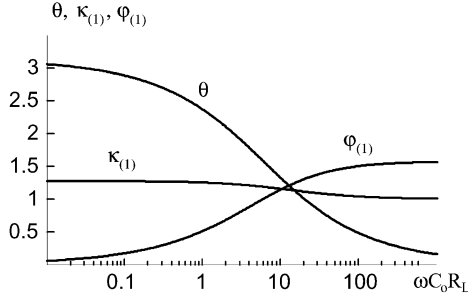


Fig. 4. VD rectifier conduction angle  $\theta$ , phase angle  $\varphi_{(1)}$  and voltage waveform coefficient  $k_{(1)}$  as a function of the PT load parameter  $\omega C_o R_L$ .

the frequency of maximum voltage transfer ratio. According to [3]

$$\omega^* = \sqrt{1 + \frac{C_r}{n^2 C_{eq}} \sin^2 \varphi_{(1)}}. \quad (8)$$

The waveform coefficient  $k_{(1)}$  and the phase angle  $\varphi_{(1)}$  of the first harmonics of the PT's output capacitance  $C_o$  voltage, referred to the instant  $\vartheta_o = 0$  [Fig. 2(a)] are

$$k_{(1)} = \frac{V_{Co(1)pk}}{V_{Co(pk)}} = \sqrt{a_{(1)}^2 + b_{(1)}^2} \quad (9)$$

$$\varphi_{(1)} = \tan^{-1} \left( \frac{a_{(1)}}{b_{(1)}} \right) \quad (10)$$

where  $V_{Co(pk)}$  is the peak value of the voltage  $v_{Co}$  (Fig. 2),  $a_{(1)}$  and  $b_{(1)}$  are the first components of the Fourier series expansion

$$a_{(1)} = -\frac{2}{\pi} \left[ \frac{\pi - \theta + 0.5 \sin(2\theta)}{1 + \cos \theta} \right] \quad (11)$$

$$b_{(1)} = \frac{2}{\pi} (1 - \cos \theta). \quad (12)$$

Fig. 4 represents the VD rectifier conduction angle  $\theta$ , the phase angle  $\varphi_{(1)}$  and the voltage waveform coefficient  $k_{(1)}$  as a function of the load parameter  $\omega C_o R_L$ .

The equivalent resistance and capacitance are [3]

$$\begin{cases} R_{eq}^{VD} = \frac{1}{8} k_{(1)}^2 R_L \\ C_{eq}^{VD} = \frac{\tan \varphi_{(1)}}{\omega R_{eq}^{VD}} \end{cases} \quad (13)$$

The voltage transfer function of the rectifier

$$k_{rect} = \frac{V_L}{V_{Co(1)pk}} = \frac{2}{k_{(1)}}. \quad (14)$$

### B. Current Doubler Rectifier

When connected to the output of the PT converter, the CD rectifier, as in the case of the halfwave rectifier [4], can operate in overlapping (OM) or nonoverlapping mode (NOM) with respect to the diodes' currents.

Fig. 5 shows the waveforms of the PT current  $i_r/n$  (referred to the secondary side of the PT), and the input current to the rectifier,  $i_{in(rect)}$  in the OM [Fig. 5(a)] and NOM [Fig. 5(b)].

We assume that the load current  $I_L$  and the inductors'  $L_1, L_2$  currents have negligible ripple and therefore the waveform  $i_{in(rect)}$  is clamped to the inductors' currents that are equal to

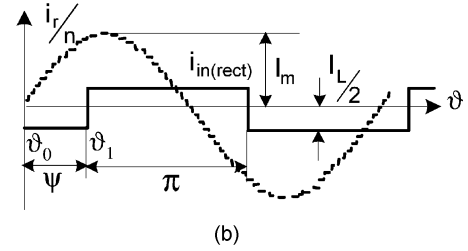
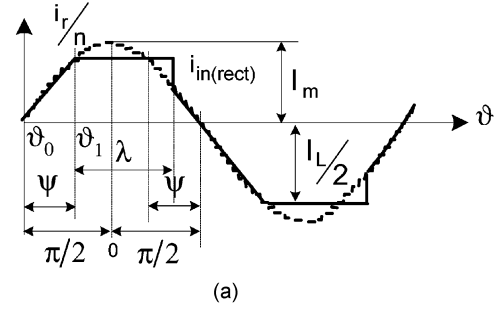


Fig. 5. Current doubler rectifier input current (solid line) and a sinusoidal PT resonant current (dotted line): (a) OM and (b) NOM.

the half the value of the load current. The difference between currents  $i_r/n$  and  $i_{in(rect)}$  is the current of the PT output capacitor  $C_o$

$$i_{Co} = I_m \sin \vartheta - 0.5 I_L \quad (15)$$

where  $I_m$  is the peak of the  $i_r/n$  current and  $\vartheta = \omega t$  is normalized time referred to the instant  $\vartheta_o$  (Fig. 5). The current  $i_{Co}$  charges and discharges the capacitor  $C_o$  during the time interval  $\lambda$  when the capacitor is not shorted through the conducting diodes. In OM [Fig. 5(a)], the capacitor current does not include a step at the instant  $\vartheta_1$  when the preceding overlapping period terminates. At this instant

$$\frac{i_r}{n} = \frac{I_L}{2} = I_m \sin \psi \quad (16)$$

where  $\psi$  is defined in Fig. 5. In NOM [Fig. 5(b)]  $i_{in(rect)}$  has a rectangular waveform. The steps of this current correspond to the instants when the capacitor voltage changes polarity.

In steady state, the average charge during the time period  $\lambda$  is zero. Therefore in OM

$$\int_{\psi}^{\psi+\lambda} (I_m \sin \vartheta - I_m \sin \psi) d\vartheta = 0. \quad (17)$$

The solution of this equation is

$$\psi = \tan^{-1} \left( \frac{1 - \cos \lambda}{\lambda - \sin \lambda} \right). \quad (18)$$

The voltage across  $C_o$  is obtained from (15) and (16). Taking into account that  $v_{Co} = 0$  at  $\vartheta = \psi$

$$v_{Co} = \frac{I_m}{\omega C_o} [\cos \psi - \cos \vartheta + (\psi - \vartheta) \sin \psi]. \quad (19)$$

The average output voltage of the rectifier is found from (19)

$$V_L = \frac{1}{2\pi} \int_{\psi}^{\psi+\lambda} v_{Co} d\vartheta. \quad (20)$$

On the other hand

$$V_L = I_L R_L = 2I_m R_L \sin \psi. \quad (21)$$

By combining (18)–(21), we derive an important equation that relates the duration  $\lambda$  of the capacitor  $C_o$  voltage pulses to the parameter  $Q\omega^* = \omega C_o R_L$

$$\frac{0.5\lambda}{\tan(0.5\lambda)} = 1 - \sqrt{2\pi Q\omega^*} \quad (22)$$

where  $\omega^*$  can be calculated from (8), which is relevant to the CD as well as to the VD rectifiers.

It follows from (22) that OM corresponds to the range of  $\omega C_o R_L < 1/2\pi$ .

Replacing the real voltage pulses  $v_{C_o}$  by an equivalent sine wave with the same duration  $\lambda$  and the same peak  $V_{C_o(pk)}$  we define  $k_{(1)}$ ,  $\varphi_{(1)}$  and  $V_L/V_{C_o(pk)}$

$$k_{(1)} = \frac{4}{\lambda} \frac{\cos(\frac{\lambda}{2})}{(\frac{\pi}{\lambda})^2 - 1} \quad (23)$$

$$\varphi_{(1)} = \psi + \frac{\lambda}{2} - \frac{\pi}{2} \quad (24)$$

$$\frac{V_L}{V_{C_o(pk)}} = \frac{\lambda}{\pi^2}. \quad (25)$$

In NOM [Fig. 5(b)]  $\lambda = \pi$

$$\frac{1}{\pi} \int_{\psi}^{\psi+\pi} \left( I_m \sin \vartheta - \frac{I_L}{2} \right) d\vartheta = 0. \quad (26)$$

It follows from this that

$$\cos \psi = \frac{\pi I_L}{4 I_m} \quad (27)$$

$$\begin{cases} k_{(1)} = 1 \\ \varphi_{(1)} = \psi \end{cases} \quad (28)$$

$$\frac{V_L}{V_{C_o(pk)}} = \frac{1}{\pi} \quad (29)$$

$$\omega C_o V_{C_o(1)pk} = I_m \sin \psi. \quad (30)$$

From (27), (29), and (30) we obtain

$$\tan \psi = 4\omega C_o R_L = 4Q\omega^*. \quad (31)$$

The duration of PT output capacitor voltage pulses  $\lambda$ , the CD rectifier voltage waveform coefficient  $k_{(1)}$ , the phase angle  $\varphi_{(1)}$ , and the conduction angle  $\psi$  as a function of  $\omega C_o R_L$  are depicted in Fig. 6.

From (9), (23), and (25) we obtain the voltage transfer ratio of the rectifier in OM

$$k_{\text{rect}} = \frac{V_L}{V_{C_o(1)pk}} = \frac{\lambda}{\pi^2 k_{(1)}}. \quad (32)$$

In NOM applying  $\lambda = \pi$  and  $k_{(1)} = 1$

$$k_{\text{rect}} = \frac{1}{\pi}. \quad (33)$$

Based on (4), (5), (9), and (25), the equivalent load resistance and capacitance in the OM [Fig. 5(a)] are

$$\begin{cases} R_{\text{eq}}^{\text{CD}} = \frac{1}{2} \left( \frac{\pi^2}{\lambda} \right)^2 k_{(1)}^2 R_L \\ C_{\text{eq}}^{\text{CD}} = \frac{\tan \varphi_{(1)}}{\omega R_{\text{eq}}^{\text{CD}}}. \end{cases} \quad (34)$$

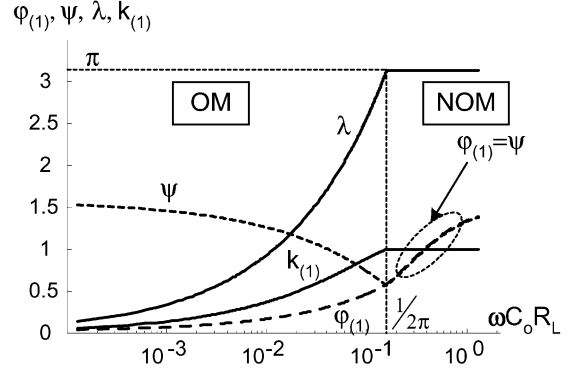


Fig. 6. CD rectifier: duration of the capacitor  $C_o$  voltage pulses  $\lambda$ , the rectifier voltage waveform coefficient  $k_{(1)}$  and phase angle  $\varphi_{(1)}$ , and the angle  $\psi$  (see Fig. 5) as a function of the PT load parameter  $\omega C_o R_L$ .

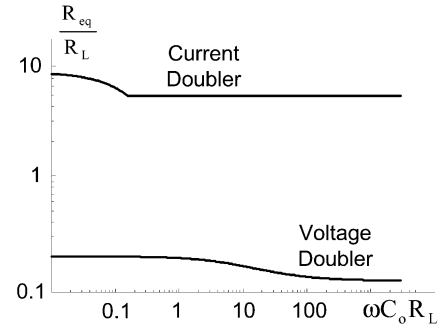


Fig. 7. Normalized equivalent resistance  $R_{\text{eq}}/R_L$  as a function of the PT load parameter  $\omega C_o R_L$  for the two rectifiers.

From (28) and (34) when  $\lambda = \pi$ , the equivalent resistance and capacitance in the NOM are found to be

$$\begin{cases} R_{\text{eq}}^{\text{CD}} = \frac{\pi^2}{2} R_L \\ C_{\text{eq}}^{\text{CD}} = \frac{\tan \varphi_{(1)}}{\omega R_{\text{eq}}^{\text{CD}}} = \frac{8}{\pi^2} C_o \end{cases} \quad (35)$$

### C. Characteristics of the Compared Rectifiers

Figs. 7–9 show the ratios  $R_{\text{eq}}/R_L$ ,  $C_{\text{eq}}/C_o$ , and the rectifier gain  $k_{\text{rect}}$  as a function of the PT load parameter  $\omega C_o R_L$  for both VD and CD rectifier's types. Fig. 7 shows that in the CD rectifier the equivalent resistance is an order of magnitude higher than  $R_L$  while in VD it is in order lower. That's why, when the load resistance is low one should use the CD rectifier to obtain better efficiency while when  $R_L$  is high a VD rectifier is more suitable. Fig. 8, demonstrates that for high load parameter  $\omega C_o R_L$  the equivalent capacitance  $C_{\text{eq}}$  of the CD rectifier is less than  $C_o$ . This means that the CD rectifier has inductive behavior in that region. Fig. 9 shows that the rectifier gain is about four times higher in the VD than in the CD.

## III. GENERAL EQUATIONS OF A PT LOADED BY AN OUTPUT RECTIFIER

For both rectifiers, the PT voltage transfer ratio at the frequency of maximum output voltage gain  $\omega^*$  (8) referred to the primary side of PT is [5]

$$k_{21m} = \frac{V_{C_o(pk)}}{nV_{\text{in}(pk)}} = \frac{1}{\cos \varphi_{(1)} + \frac{1}{K_{\text{PT}} \cos \varphi_{(1)}}} \quad (36)$$

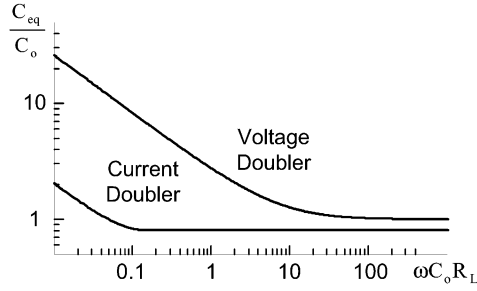


Fig. 8. Normalized equivalent capacitance  $C_{eq}/C_o$  as a function of the PT load parameter  $\omega C_o R_L$  for the two rectifiers.

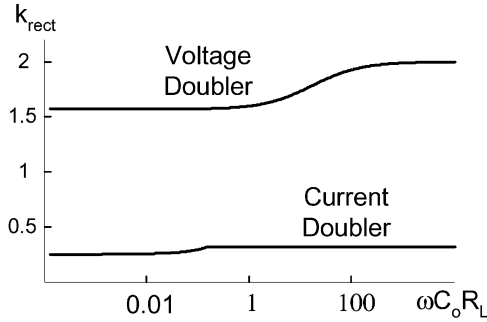


Fig. 9. VD and CD rectifier voltage gain as a function of the PT load parameter  $\omega C_o R_L$ .

where  $V_{in(pk)}$  is the peak input voltage.

As proven in [3]:  $1 < \omega^* < 1.1$ . For such a narrow frequency range, the changes in the values of the parameters  $\varphi_{(1)}$  and  $C_{eq}$  are insignificantly small. Consequently,  $\omega^*$  was obtained under the assumption that the values of  $\varphi_{(1)}$  and  $C_{eq}$  are independent of  $\omega$ .

The dc output to peak input voltage transfer ratio  $k_o$  is

$$k_o = \frac{V_o}{V_{in(pk)}} = nk_{21m}k_{rect}. \quad (37)$$

The efficiency of the PT for both rectifiers is given by [5]

$$\eta_{PT} = \frac{1}{1 + \frac{R_m}{R_{eq}''}} = \frac{1}{1 + \frac{R_L}{K_{PT} R_{eq} \cos \varphi_{(1)}}}. \quad (38)$$

The ratio of the output power  $P_o$  to the power dissipation of the PT  $P_{PD}$  for the both rectifiers is thus

$$\Delta_{PT} = \frac{P_o}{P_{PD}} = \frac{\eta_{PT}}{1 - \eta_{PT}} = \frac{R_{eq}}{R_L} K_{PT} \cos \varphi_{(1)}. \quad (39)$$

In the case of nonideal rectifier one should take into account the diodes' losses.

The rectifiers' efficiency is

$$\eta_{rect} = \frac{1}{1 + \frac{P_D}{P_o}} \quad (40)$$

where  $P_D$  are diodes' power losses.

The diodes' power losses in both rectifiers are approximated by

$$P_D = 2 \left( I_{D(ave)} V_F + I_{D(rms)}^2 R_s \right) \quad (41)$$

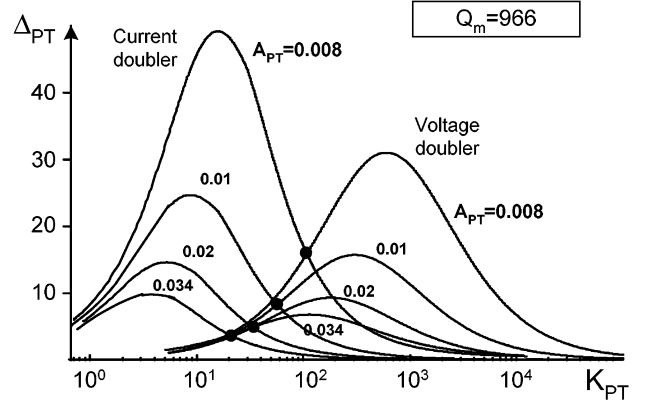


Fig. 10. The ratio of the output power  $P_o$  to the PT power dissipation  $P_{PD}(\Delta_{PT})$  as a function of the normalized load resistance  $K_{PT} = R_L/n^2 R_m$  for different PT factors  $A_{PT} = \omega R C_o R_m n^2$ . Plots are for mechanical quality factor  $Q_m = 966$ .

where  $I_{D(ave)}$  is the average diode current,  $V_F$  is the forward diode voltage,  $I_{D(rms)}$  is the effective diode current and  $R_s$  is the diode's incremental resistance. In the CD rectifier  $I_{D(ave)} = 0.5I_L$ , where  $I_L$  is load current. In the VD rectifier  $I_{D(ave)} = I_L$ .

The efficiency of the rectifiers when connected at the PT output is found to be

$$\eta_{rect}^{CD} \approx \frac{1}{1 + \frac{V_F}{V_L} \left[ 1 + \left( \frac{I_{D(rms)}}{I_{D(ave)}} \right)^2 \frac{V_L R_s}{V_F 2R_L} \right]} \quad (42)$$

$$\eta_{rect}^{VD} \approx \frac{1}{1 + \frac{2V_F}{V_L} \left[ 1 + \left( \frac{I_{D(rms)}}{I_{D(ave)}} \right)^2 \frac{V_L R_s}{V_F R_L} \right]} \quad (43)$$

where  $V_L$  is the average load voltage and  $(I_{D(rms)})/(I_{D(ave)})$  is the ratio of rms and the average diodes' currents

$$\left. \frac{I_{D(rms)}}{I_{D(ave)}} \right|_{CD} = \sqrt{\frac{1}{\pi} \left\{ \left[ \frac{\lambda^2}{\pi^2} + \frac{2}{3} \left( 1 - \frac{\lambda^2}{\pi^2} \right)^2 \right] (\pi - \lambda) + \lambda \right\}} \quad (44)$$

$$\left. \frac{I_{D(rms)}}{I_{D(ave)}} \right|_{VD} = \sqrt{\frac{\pi \left[ \theta - \frac{1}{2} \sin(2\theta) \right]}{[1 - \cos(\theta)]^2}}. \quad (45)$$

Taking into account the rectifier losses, the overall efficiency will be

$$\eta = \eta_{rect} \eta_{PT}. \quad (46)$$

#### IV. MAIN COMPARISON RESULTS

Fig. 10, that is based on (38), (39) shows the power handling capability  $\Delta_{PT}$  as a function of the normalized load factor  $K_{PT} = R_L/n^2 R_m$  for different values of the normalized PT parameter  $A_{PT} = \omega_r C_o n^2 R_m$ . Since the efficiency as it follows from (39) equals  $\Delta_{PT}/(\Delta_{PT} + 1)$  the maximum of  $\Delta_{PT}$  corresponds to the point of maximum efficiency. The generic data of Fig. 10 suggest that for any given PT (i.e., a specific  $A_{PT}$ ) the efficiency that can be achieved with a CD rectifier is higher than the one that can be reached with the VD rectifier. The data also show, as expected, that for a given PT, the load resistance  $R_L$

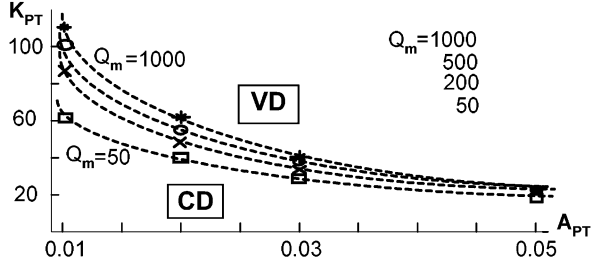


Fig. 11. Boundaries between preferred operating regions that provide higher efficiency for VD and CD rectifiers for the different values of the mechanical quality factor  $Q_m$ .

that corresponds to maximum efficiency, is lower in the CD rectifier than in the VD rectifier. That is, for a given PT, maximum efficiency will be obtained in the VD rectifier at higher voltages than in the CD rectifier. From Fig. 10 one can recognize the borderline between load values that will produce a higher efficiency with a CD rectifier, to the load range that is more compatible to the VD rectifier (from the efficiency point of view). Fig. 11, built from Fig. 10, delineates the borderline between the CD and VD regions for different PTs for a range of  $A_{PT}$  values. This plot can be used as a tool for selecting the rectifier for a given load conditions of a given PT. This figure implies that, for a given PT, one should use a VD rectifier when the load factor  $K_{PT}$  is higher than the dotted line, and CD—when the load factor is lower. The plots (Fig. 10) are built for mechanical quality factor of PT  $Q_m = 966$ . For larger values of  $Q_m$ , the  $\Delta_{PT}$  does not change significantly.

If the high voltage gain is to be achieved in a given application, it follows from (9), (14), (23), (32), and (33) that the VD has higher  $k_{rect}$  than CD, therefore VD is better choice for a given PT.

It is further found in this study that for low load resistances, higher voltage transfer ratios  $k_o$  can be obtained when using the CD rather than the VD rectifier. This is because the efficiency of CD with low load resistances is higher than the VD. In addition, the efficiency of CD rectifier  $\eta_{rect}^{CD}$  is higher than VD  $\eta_{rect}^{VD}$ , because the ratio of  $I_{D(rms)}/I_{D(ave)}$  in the CD is lower than in the VD.

## V. SIMULATION AND EXPERIMENTAL RESULTS

### A. Estimating the Parameters of the PT Equivalent Circuit

Considering the fact that PT is a nonlinear element, a linear network can model its behavior only over small frequency and current/voltage ranges. Parameter extraction measurements were therefore carried out around the operational frequency of the device and around the nominal current levels. Tests runs have shown that this particular device is not that sensitive to the voltage level.

Measurements were carried out from the input and output sides while the complementary terminals were shorted. The equivalent circuit parameters of experimental PT were obtained as follows.

- 1) The total input and output capacitances  $C_{Tin}$  and  $C_{To}$  were measured at low frequencies. These capacitances include in addition to  $C_{in}$  and  $C_o$  also the series capacitance

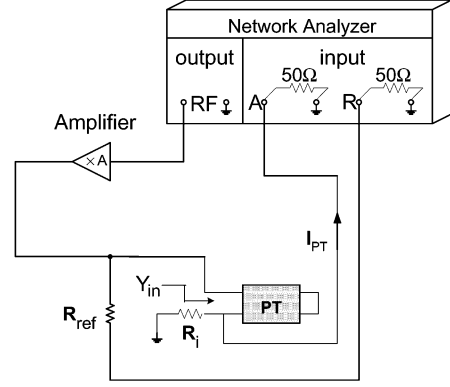


Fig. 12. Experimental setup of network analyzer measurements.  $R_{ref} = 466 \Omega$ ,  $R_i = 1 \Omega$ .

$C_T$  and all parasitic capacitances in parallel to the series network  $C_T-L_T-R_m$ .

- 2) The input admittance  $Y_{in}$  (magnitude and phase) was obtained by the setup shown in Fig. 12 applying the HP4395A network analyzer. The input rms voltage of PT was around  $V_{in} = 3$  V to keep the input current within the operational range of the device (250 mA). The frequency was swept from 100 to 150 kHz. The measured data  $V_A/V_R$  (Fig. 12) was recalculated to find the actual magnitude of admittance of PT by

$$Y_{in} = \frac{50+R_i}{(50+R_{ref})R_i} \frac{V_A}{V_R} \frac{1}{1 - \frac{50}{50+R_{ref}} \frac{V_A}{V_R}} \quad (47)$$

where experimental  $R_i = 1 \Omega$  and  $R_{ref} = 466 \Omega$ .

- 3) The resonant  $f_r$  and anti-resonant  $f_a$  frequencies, corresponding to the zero imaginary part of the admittance, were found for both input and output terminals (in/o), respectively.
- 4) Input and output capacitances were estimated from the measured values of  $C_T$ ,  $f_r$ , and  $f_a$  [7]

$$C_{(in/o)} = \left( \frac{f_r(in/o)}{f_a(in/o)} \right)^2 C_{T(in/o)}. \quad (48)$$

This equation is valid when the quality factor  $Q_m$  of the PT is sufficiently high ( $Q_m > 300$ ), and if the parasitic capacitances parallel to the  $R_m-C_T-L_T$  and  $C_{in}$  network are negligibly small.

- 5) The series circuit parameters  $C_T-L_T-R_m$  (in/o) were calculated from the measured magnitude and the phase of the admittance of each side by the method presented in [8] that is based on two admittances values slightly before the resonant frequency.
- 6) The transfer ratio  $n$  of PT was extracted from the calculated values of the series inductances obtained from the input and output measurements

$$n = \sqrt{\frac{L_{r(out)}}{L_{r(in)}}}. \quad (49)$$

The equivalent parameters of the experimental PT (a radial vibration mode PT, Face Co., VA, USA) were found to be as follows.  $C_{in} = 1.72$  nF,  $C_o = 1.33$  nF,  $L_r = 10.5$  mH,  $C_r = 172.5$   $\mu$ F,  $R_m = 21 \Omega$ ,  $n = 1.08$ . Thus, the series resonant frequency of PT is calculated to be 118.3 kHz, the mechanical

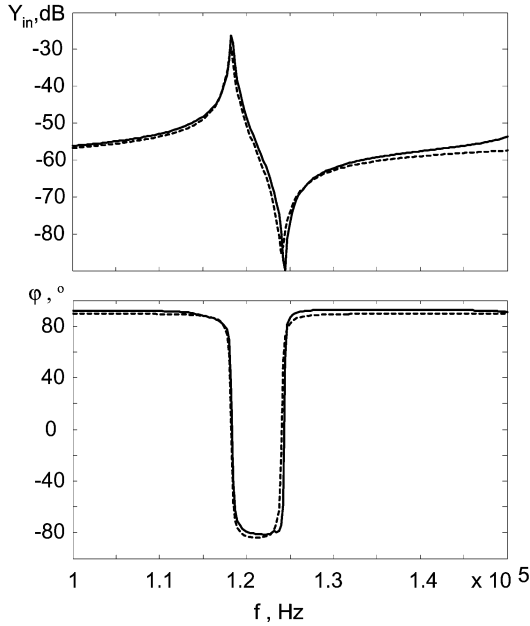


Fig. 13. Input admittance (upper—magnitude, lower—phase) of the experimental PT. Solid line—measured, dotted line—reconstructed by simulation of PT equivalent circuit based on the calculated equivalent circuit parameters.

quality factor (3) is  $Q_m = 371.5$ , and the normalized PT factor (2) is  $A_{PT} = 0.0242$ .

Fig. 13 shows the measured admittance (magnitude and phase) and the reconstructed admittance obtained by PSPICE simulation of the PT equivalent circuit applying the estimated model parameters. The slight difference between experimental and reconstructed curves in the region of antiresonant frequency is probably the result of inaccuracy in the estimation of the input capacitance  $C_{in}$ . An error in the value of this capacitance has a larger effect on  $f_A$  than on  $f_r$  because of the high impedance of the network at the antiresonant region. The value of  $C_{in}$  can be corrected by an iteration but this is not deemed essential in present case, because the nominal operational region of the PT is near  $f_r$  where the matching between the measured and reconstructed admittance is excellent.

### B. Measuring the Voltage Ratio and Efficiency of PT With CD and VD Rectifiers

The experimental setup included a LeCroy WaveRunner Scope LT264M DSO with APO15 Current Probe, using the PMA1 Power Measure Analysis Software for calculating the input power of the PT. The experiments were carried out in the maximum output voltage mode with frequency adjusting.

The output power of CD converter was varied from 4 to 11 W, keeping mostly around 6 to 7 W. Load resistances were varied from 30  $\Omega$  to 10 k $\Omega$ , that corresponds to the  $K_{PT}$  values from 1.22 to 410, respectively. In order to prevent the PT from overheating the input current of CD converter was limited to 250 mA (rms).

The output voltage of the VD converter was kept constant at  $V_L = 170$  V for the loads values from 2 k $\Omega$  to 100 k $\Omega$ . For lower resistances range, the current conditions were kept similar to the CD case.

Figs. 14–15 show the experimental and simulation results as well as the calculated results according to the model presented

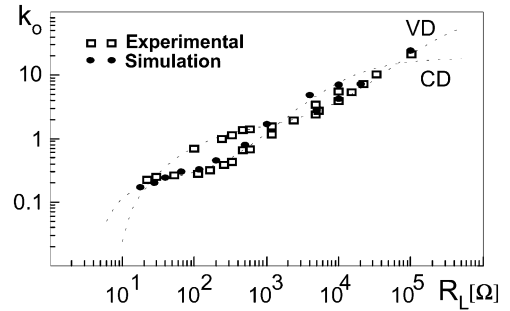


Fig. 14. Theoretical prediction (dotted lines), experimental and simulation results of output to input voltage ratio of the PT converter for the two rectifiers' types as a function of the load resistance. Normalized parameters:  $A_{PT} = 0.0242$ ,  $Q_m = 371.5$ ,  $K_{PT}$  varies from 0.5 to  $3 \cdot 10^5$ .

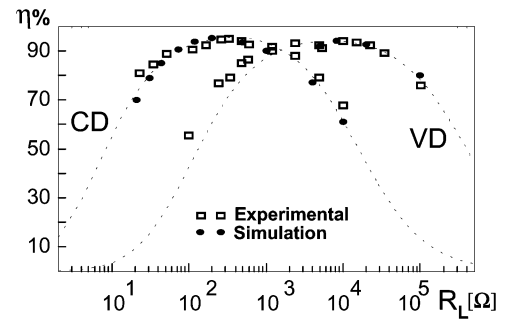


Fig. 15. Theoretical prediction (dotted lines), experimental and simulation results of the efficiency of the PT converter with VD and CD rectifiers as a function of the load resistance  $R_L$ . Normalized parameters: as in Fig. 14.

here: the output to input voltage transfer ratio (Fig. 14), and the converter efficiency (Fig. 15) as a function of the load resistance. Note, that efficiency (Fig. 15) was calculated with the assumptions that the forward diodes voltage  $V_F$  is constant in the operating current range and that the diode's incremental resistance  $R_s$  is negligibly small. Under the experimental conditions the forward voltage of the MUR440  $V_F$ , was about 0.7 V for most of the measurements and therefore this value was chosen in diode loss calculations. In general, good agreement was found between the experimental, simulation and theoretical results (Figs. 14 and 15).

## VI. CONCLUSION

This study carries out a comprehensive comparison of two popular rectifiers in PT power converter: a current doubler and a voltage doubler. The advantages and disadvantages of each rectifier configuration were studied resulting in a recommendation of the preferred applications areas for each rectifier in terms of output current and voltage, power handling capability, load resistance etc.

The results of this study are general and are not confined to any particular PT since we apply here generic parameters for the PT and load. The PT is characterized by the normalized parameters:  $A_{PT}$ ,  $Q_m$ , and  $n$ , while the load is expressed in a normalized form as  $K_{PT}$ . These fundamental parameters are used to develop the relationship for the maximum voltage transfer function and  $\Delta_{PT}$  (that is the ratio of the output power to the power dissipated by the PT). Since the maximum allowable PT power dissipation is one of the most important design constrains, the

value of the parameter  $\Delta_{PT}$  in any given application will determine what would be the maximum output power of the system.

The study shows that for low load resistances  $R_L$  higher voltage transfer ratios can be obtained when using the CD rather than the VD rectifier whereas for achieving high gain the VD rectifier is much more suitable (Fig. 14).

In general, the simulations and the experiments confirm the theoretical analysis and were found to be in a good agreement. The discrepancies that are observed in some cases are probably due to experimental error.

The analytical methodology developed and applied in this paper and the closed form analytical expressions that were derived, provide generic information on PT converter that apply the CD and VD rectifiers. The analytical expressions that are also summarized in generic graphs shed some more light on characteristics and advantages and disadvantages of PTs. As such, they could be useful both ways: when selecting a PT for a given application and when designing a PT for a specific system.

#### REFERENCES

- [1] R. L. Steigerwald, "A comparison of half-bridge resonant converter topologies," *IEEE Trans. Power Electron.*, vol. 3, pp. 174–182, Apr. 1988.
- [2] G. Ivensky, A. Kats, and S. Ben-Yaakov, "An RC load model of parallel and series-parallel resonant converters with capacitive output filter," *IEEE Trans. Power Electron.*, vol. 14, pp. 515–521, May 1999.
- [3] G. Ivensky, M. Shvartsas, and S. Ben-Yaakov, "Analysis and modeling of a voltage doubler rectifier fed by a piezoelectric transformer," *IEEE Trans. Power Electron.*, vol. 19, pp. 542–549, Mar. 2004.
- [4] G. Ivensky, S. Bronstein, and S. Ban-Yaakov, "Analysis and design of a piezoelectric transformer ac/dc converter in a low voltage application," in *Proc. IEEE PESC*, 2002, pp. 409–414.
- [5] G. Ivensky, I. Zafrany, and S. Ban-Yaakov, "Generic operational characteristics of piezoelectric transformers," *IEEE Trans. Power Electron.*, vol. 17, pp. 1049–1057, Nov. 2002.
- [6] S. Hamamura, D. Kurose, T. Ninomia, and M. Yamamoto, "Piezoelectric transformer ac–dc converter over a worldwide range of input voltage by combined PWM and PFM control," in *Proc. IEEE PESC*, 2001, pp. 416–421.
- [7] C. Y. Lin, "Design and analysis of piezoelectric transformer converters," Ph.D. dissertation, Virginia Polytech. Inst. State Univ., Blacksburg, July 1997.
- [8] S. Ben-Yaakov and N. Krihely, "Modeling and driving piezoelectric resonant blade elements," in *Proc. IEEE APEC*, 2004, pp. 1733–1739.



**Gregory Ivensky** was born in Leningrad, Russia, in 1927. He received the Energy Engineer Diploma from the Leningrad Railway Transport Institute in 1948 and the Candidate and Dr.Tech.Sci. degrees from the Leningrad Polytechnic Institute, in 1958 and 1977, respectively.

From 1951 to 1962, he was at the Central Design Bureau of Ultrasound and High Frequency Devices, Leningrad. From 1962 to 1989, he was at the North-Western Polytechnic Institute, Leningrad, where in 1980 he became a Full Professor in the Department of Electronic Devices. Since 1991, he has been a Professor at the Department of Electrical and Computer Engineering, Ben-Gurion University of the Negev, Beer-Sheva, Israel. His research interests include rectifiers, inverters, dc-dc converters, EMI and power quality issues, and induction heating.



**Svetlana Bronstein** was born in Leningrad, Russia. She received the Electric Engineer Diploma from the Leningrad Polytechnic Institute in 1984 and is currently pursuing the Ph.D. degree at the Ben-Gurion University of the Negev, Beer-Sheva, Israel.

From 1984 to 1991, she worked in the Mendelev Research-Engineering Institute of Metrology, Leningrad. Her areas of interests include piezoelectric transformers in power electronics, dc-dc resonant power converters, and modeling and simulation.



**Shmuel (Sam) Ben-Yaakov** (M'87) was born in Tel Aviv, Israel, in 1939. He received the B.Sc. degree in electrical engineering from the Technion, Haifa, Israel, in 1961 and the M.S. and Ph.D. degrees in engineering from the University of California Los Angeles, in 1967 and 1970, respectively.

He is presently a Professor with the Department of Electrical and Computer Engineering, Ben-Gurion University of the Negev, Beer-Sheva, Israel, and heads the Power Electronics Group, and was Chairman of that department from 1985 to 1989. He serves as Chief Scientist of Green Power Technologies, Ltd., Israel, and is a Consultant to commercial companies on various subjects, including analog circuit design and power electronics. His current research interests include power electronics, circuits and systems, electronic instrumentation, and engineering education.